

Supplementary Information

2. Experimental

2.1. X-ray crystal refinement

The diffraction data was collected with a Bruker SMART APEX CCD diffractometer using monochromatic Mo-K α radiation ($\lambda=0.71073 \text{ \AA}$) at 100 (2) K. The linear absorption coefficients and the anomalous dispersion corrections were mentioned from the International Tables for X-ray crystallography [1]. Using Olex2, the structure was solved with the olex2.solve [2] structure solution program using Charge Flipping and refined with the olex2.refine [2] refinement package using Gauss-Newton minimisation. All hydrogen atoms were located in difference Fourier maps in the structures and refined isotropically. All non-H atoms were refined anisotropically.

2.2. Topological Analysis

The analysis was performed with the topcryst.com [3]. The RCSR three-letter codes [4] were used to designate the network topologies. Those nets, that are absent in the RCSR, are designated with the TOPOS NDn nomenclature [5], where N is a sequence of coordination numbers of all non-equivalent nodes of the net, D is periodicity of the net (D=M, C, L, T for 0-,1-,2-,3-periodic nets), and n is the ordinal number of the net in the set of all non-isomorphic nets with the given ND sequence. To calculate the underlying nets, we used algorithms [5], the application of which for specific structures is discussed in the article [6]. The TTD collection [7] was used to determine the topological type of the crystal structure.

2.3. Computational details

Among the numerous quantum-computing techniques, the Density Functional Theory (DFT) is a useful tool for describing key molecular characteristics. The B3LYP approach and 6-311++G(d,p) basis set [8,9] supplied in the Gaussian 03W and Gauss View [10] were used for the most of the computational calculations, and some of the findings were also acquired via ORCA (4.0.1) [11]. Geometrical bond parameters, vibrational wave numbers, HOMO-LUMO energy gap and molecular electrostatic potential (MEP) are molecular properties that were all achieved by the optimized molecular structure. The Swiss ADME tool [12] provides a molecule with an active substance-like property, which is required for synthesis of active compounds. Visualization was done with Multiwfn software [13], graph plotting was carried out by Origin8.0 programme [14]. IP and EA were estimated using Koopman's theorem, i.e. EA= - ELUMO and IP= -EHOMO [15] and chemical reactivity descriptors were derived using IP and EA by adopting the formulas given below.

$$\text{Electro-negativity } (\chi) = \frac{IA+EA}{2}, \text{ Chemical potential } (\mu) = \frac{-(IA+EA)}{2}$$

$$\text{Chemical hardness } (\eta) = \frac{-IA-EA}{2}$$

$$\text{Chemical softness } (\sigma) = \frac{1}{2\eta}, \text{ Electrophilicity index } (\omega) = \frac{\mu*\mu}{2\eta}$$

Hirshfeld surface analysis was used to determine the intramolecular and intermolecular interconnections inside the crystal surface, as well as the H-bonded interactions. It is a useful technique for analysing unit cell packing in crystal. The study is based on a 3-D graphical representation in the geographical region where the molecule interacts with nearby molecules, and 2-D fingerprint images that describes the kind of atomic interaction. This analysis was used to study crystals qualitatively and quantitatively [16,17]. The Crystal Explorer 17 software [18] was applied to record the Hirshfeldsurface and fingerprint. Eq. [19] may be used to determine the mapping of the normalised contact (d_{norm}).

$$d_{norm} = \frac{d_i - r_i^{vdw}}{r_i^{vdw}} + \frac{d_e - r_e^{vdw}}{r_e^{vdw}}$$

r_i^{vdw} and r_e^{vdw} represents the radii of atoms (van der waals). The distance from the surface to the closest nucleus d_i (internal) and d_e (external) to the atom were used to analyze the interactions in crystals. 3-D Hirshfeld surface images rendered in the Hirshfeld surface as d_{norm} , with a red colour area corresponding to negative d_{norm} side and a near intermolecular interaction, and a blue color area corresponds positive d_{norm} value and longer intermolecular interactions. The zero d_{norm} value is represented by the white portion. The d_i and d_e ends in the 2-D fingerprint diagram indicate a sort of intermolecular interactions that exists inside the crystal's molecules [20].

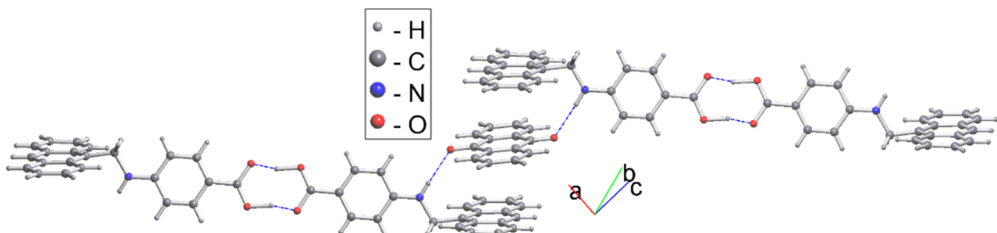


Figure S1. The structural fragments of molecular structure of L3

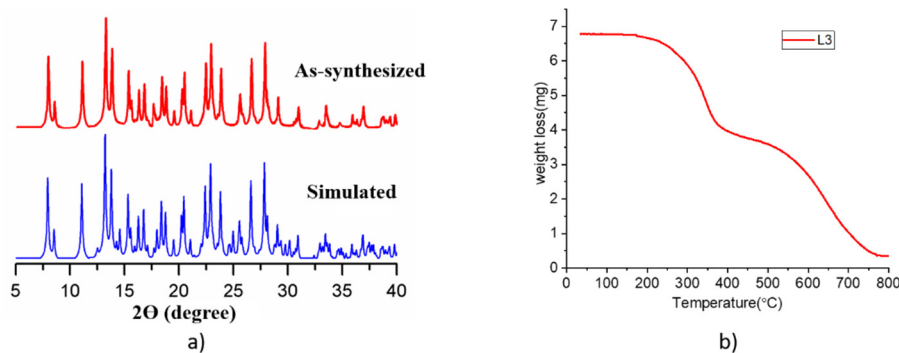


Figure S2. (a) Simulated and As-synthesized PXRD of L3, **(b)** TGA curve of L3

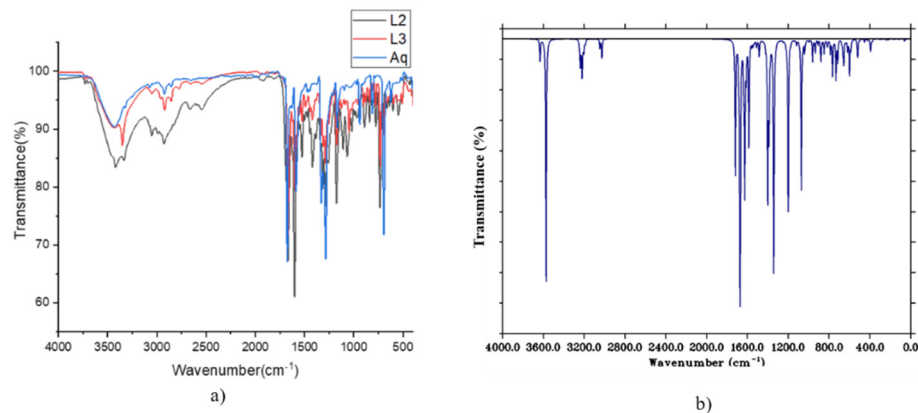


Figure S3 (a) Experimental FTIR spectra of L2, L3 and Anthraquinone, (b) Simulated FTIR spectrum of L3

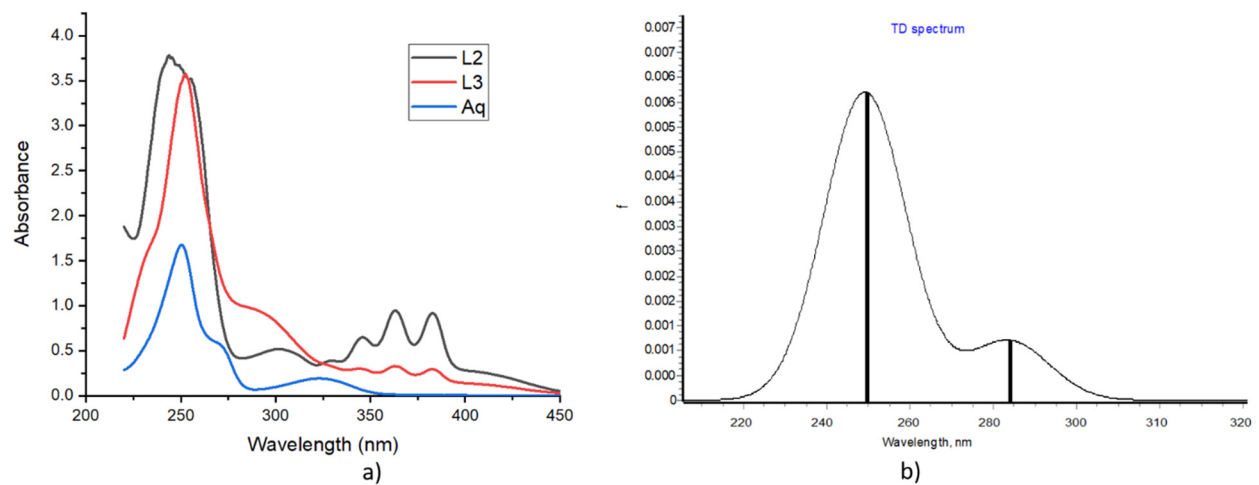


Figure S4 (a) Experimental UV-Visible spectra of L2 and L3, (b) UV-visible spectrum of L3 obtained through TD-DFT calculations

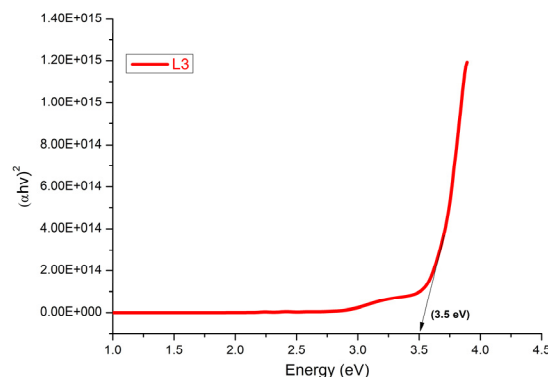


Figure S5. Tauc's plot showing band gap

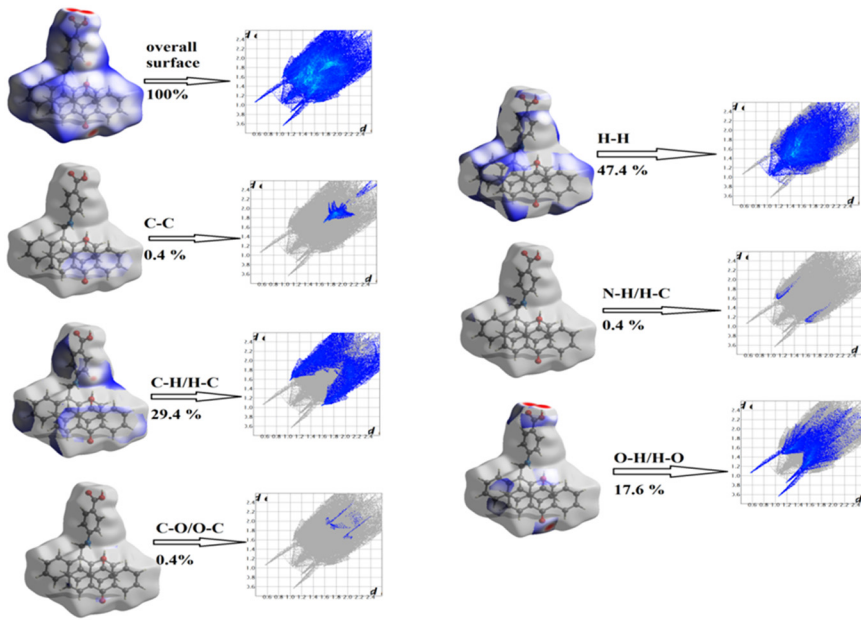


Figure S6. 2-D fingerprint plot of different dnorm contributions for L3

Table S1. Bond Lengths for L3

Atom	Atom	Length/ \AA	Atom	Atom	Length/ \AA
O1	C1	1.280 (2)	C13	C14	1.353 (3)
O2	C1	1.277 (2)	C14	C15	1.426 (3)
O3	C23	1.225 (2)	C15	C16	1.391 (3)
N1	C5	1.357 (2)	C16	C17	1.390 (3)
N1	C8	1.453 (2)	C17	C18	1.429 (3)
C1	C2	1.464 (2)	C17	C22	1.439 (3)
C2	C3	1.395 (3)	C18	C19	1.351 (3)
C2	C7	1.404 (3)	C19	C20	1.420 (3)
C3	C4	1.371 (3)	C20	C21	1.357 (3)
C4	C5	1.412 (3)	C21	C22	1.431 (3)
C5	C6	1.413 (3)	C23	C24	1.487 (3)
C6	C7	1.370 (3)	C23	C29 ¹	1.480 (3)
C8	C9	1.509 (2)	C24	C25	1.388 (3)
C9	C10	1.410 (3)	C24	C29	1.404 (3)
C9	C22	1.407 (3)	C25	C26	1.382 (3)
C10	C11	1.436 (3)	C26	C27	1.384 (4)
C10	C15	1.436 (3)	C27	C28	1.372 (3)
C11	C12	1.356 (3)	C28	C29	1.394 (3)
C12	C13	1.417 (3)			

¹1-X,1-Y,1-Z

Table S2. Bond Angles for L3

Atom	Atom	Atom	Angle/ $^{\circ}$	Atom	Atom	Atom	Angle/ $^{\circ}$
------	------	------	-------------------	------	------	------	-------------------

C8	N1	C5		121.88(15)	C16	C15	C10		118.91(18)
O2	C1	O1		122.25(17)	C16	C15	C14		121.98(18)
C2	C1	O1		118.96(16)	C17	C16	C15		122.29(18)
C2	C1	O2		118.79(16)	C18	C17	C16		121.95(18)
C3	C2	C1		121.49(16)	C22	C17	C16		119.04(18)
C7	C2	C1		120.08(16)	C22	C17	C18		118.99(18)
C7	C2	C3		118.43(17)	C19	C18	C17		121.44(19)
C4	C3	C2		121.31(17)	C20	C19	C18		119.90(19)
C5	C4	C3		120.37(17)	C21	C20	C19		120.8(2)
C4	C5	N1		122.25(16)	C22	C21	C20		121.61(19)
C6	C5	N1		119.39(16)	C17	C22	C9		119.55(17)
C6	C5	C4		118.35(17)	C21	C22	C9		123.24(17)
C7	C6	C5		120.38(17)	C21	C22	C17		117.20(17)
C6	C7	C2		121.15(17)	C24	C23	O3		121.0(2)
C9	C8	N1		112.13(15)	C29 ¹	C23	O3		120.6(2)
C10	C9	C8		119.43(17)	C29 ¹	C23	C24		118.33(18)
C22	C9	C8		120.24(17)	C25	C24	C23		120.0(2)
C22	C9	C10		120.25(17)	C29	C24	C23		120.57(19)
C11	C10	C9		122.80(18)	C29	C24	C25		119.5(2)
C15	C10	C9		119.78(18)	C26	C25	C24		120.3(2)
C15	C10	C11		117.42(18)	C27	C26	C25		120.1(2)
C12	C11	C10		121.2(2)	C28	C27	C26		120.3(2)
C13	C12	C11		120.9(2)	C29	C28	C27		120.5(2)
C14	C13	C12		120.06(19)	C24	C29	C23 ¹		121.09(19)
C15	C14	C13		121.3(2)	C28	C29	C23 ¹		119.6(2)
C14	C15	C10		119.09(18)	C28	C29	C24		119.3(2)

¹1-X,1-Y,1-Z

Table S3. Fractional Atomic Coordinates ($\times 10^4$) and Equivalent Isotropic Displacement Parameters ($\text{\AA}^2 \times 10^3$) for L3. U_{eq} is defined as 1/3 of the trace of the orthogonalised U_{ij} tensor

Atom	X	y	z	U(eq)
O1	12894.5 (16)	4.7 (12)	90.2 (11)	20.8 (3)
O2	14365.7 (16)	903.1 (13)	742.4 (12)	22.1 (3)
O3	7441.7 (18)	3892.5 (14)	3979.5 (14)	32.6 (4)
N1	7111.2 (19)	2553.0 (14)	2569.1 (14)	18.0 (4)
C1	12984 (2)	644.7 (16)	640.9 (15)	15.3 (4)
C2	11451 (2)	1103.9 (17)	1166.7 (16)	16.0 (4)
C3	9916 (2)	809.6 (17)	1130.3 (16)	18.1 (4)
C4	8477 (2)	1260.8 (17)	1603.3 (16)	17.7 (4)
C5	8515 (2)	2052.2 (17)	2129.1 (16)	15.6 (4)
C6	10071 (2)	2341.6 (17)	2176.1 (17)	17.9 (4)
C7	11498 (2)	1871.3 (17)	1709.7 (16)	17.4 (4)

C8	5525 (2)	2156.1 (18)	2709.9 (17)	17.8 (4)
C9	4145 (2)	2858.0 (17)	3198.1 (17)	16.8 (4)
C10	3887 (2)	2464.4 (17)	4424.8 (17)	18.2 (4)
C11	4997 (3)	1491.4 (18)	5245.4 (18)	22.8 (4)
C12	4711 (3)	1136.8 (19)	6420.5 (18)	28.3 (5)
C13	3289 (3)	1704 (2)	6878.0 (19)	30.9 (5)
C14	2207 (3)	2624.1 (19)	6140.1 (18)	26.1 (5)
C15	2468 (2)	3048.4 (18)	4897.3 (17)	19.5 (4)
C16	1369 (2)	3994.2 (17)	4127.1 (17)	19.7 (4)
C17	1626 (2)	4421.2 (17)	2914.9 (17)	18.6 (4)
C18	478 (3)	5381.6 (18)	2129.3 (19)	25.0 (5)
C19	745 (3)	5794.1 (19)	952.1 (19)	28.4 (5)
C20	2201 (3)	5278.3 (19)	473.4 (19)	27.8 (5)
C21	3316 (3)	4353.2 (18)	1184.7 (17)	21.0 (4)
C22	3070 (2)	3860.2 (17)	2436.2 (17)	17.0 (4)
C23	6328 (3)	4399.1 (19)	4442.7 (19)	24.4 (5)
C24	5089 (3)	5445.6 (18)	3724.4 (18)	23.8 (5)
C25	5194 (3)	5870 (2)	2509 (2)	33.0 (5)
C26	4040 (3)	6838 (2)	1835 (2)	39.4 (6)
C27	2770 (3)	7389 (2)	2370 (2)	41.2 (6)
C28	2658 (3)	6988 (2)	3570 (2)	33.0 (5)
C29	3811 (3)	6014.5 (18)	4264.5 (19)	24.6 (5)

Table S4. Anisotropic Displacement Parameters ($\text{\AA}^2 \times 10^3$) for L3. The Anisotropic displacement factor exponent takes the form: $-2\pi^2[h^2a^{*2}U_{11}+2hka^*b^*U_{12}+\dots]$

Atom	U₁₁	U₂₂	U₃₃	U₁₂	U₁₃	U₂₃
O1	18.6 (7)	25.0 (8)	24.6 (7)	-2.2 (6)	1.3 (6)	-17.1 (6)
O2	12.4 (7)	32.1 (9)	26.3 (8)	-4.1 (6)	0.6 (6)	-16.5 (7)
O3	22.5 (8)	43.1 (10)	49.1 (10)	-9.1 (7)	6.0 (7)	-35.5 (8)
N1	12.5 (8)	20.6 (9)	27.6 (9)	-3.7 (7)	1.8 (7)	-16.5 (7)
C1	15.1 (9)	15.3 (10)	13.0 (9)	-0.7 (7)	-2.3 (7)	-3.9 (8)
C2	14.7 (9)	17.1 (10)	14.8 (9)	-1.6 (8)	-0.5 (7)	-6.0 (8)
C3	19.2 (10)	20.0 (11)	19.6 (10)	-2.9 (8)	-1.9 (8)	-12.4 (8)
C4	13.2 (9)	21.3 (11)	21.8 (10)	-4.4 (8)	-1.6 (8)	-10.9 (8)
C5	15.0 (9)	16.3 (10)	13.7 (9)	-0.1 (7)	-2.9 (7)	-5.1 (8)
C6	15.8 (10)	19.5 (10)	23.9 (10)	-2.8 (8)	-2.4 (8)	-13.9 (8)
C7	13.2 (9)	20.3 (11)	21.2 (10)	-3.8 (8)	-2.2 (8)	-10.1 (8)
C8	13.1 (9)	21.0 (11)	21.9 (10)	-3.1 (8)	-0.7 (8)	-11.1 (8)
C9	13.4 (9)	18.5 (10)	23.4 (10)	-5.9 (8)	0.7 (8)	-12.3 (8)
C10	14.7 (9)	19.4 (11)	24.9 (10)	-7.1 (8)	0.1 (8)	-11.5 (8)

C11	21.3 (11)	20.5 (11)	27.4 (11)	-6.0 (8)	-3.5 (9)	-8.9 (9)
C12	34.6 (12)	23.2 (12)	26.3 (11)	-10.5 (10)	-10.1 (10)	-4.6 (9)
C13	45.6 (14)	33.3 (13)	19.3 (11)	-20.3 (11)	0.4 (10)	-10.3 (10)
C14	29.1 (12)	29.9 (12)	25.7 (11)	-12.3 (10)	7.0 (9)	-16.4 (10)
C15	19.4 (10)	21.0 (11)	23.1 (10)	-8.9 (8)	2.9 (8)	-12.3 (9)
C16	14.0 (10)	22.8 (11)	29.4 (11)	-5.8 (8)	4.6 (8)	-17.7 (9)
C17	15.9 (9)	16.0 (10)	27.2 (11)	-5.0 (8)	-0.2 (8)	-11.0 (8)
C18	17.8 (10)	21.4 (11)	37.4 (12)	1.4 (8)	-3.6 (9)	-15.2 (10)
C19	27.5 (12)	20.5 (11)	33.3 (12)	1.1 (9)	-11.9 (10)	-7.2 (10)
C20	35.0 (12)	25.2 (12)	21.4 (11)	-8.7 (10)	-4.1 (9)	-5.5 (9)
C21	22.2 (10)	21.7 (11)	22.0 (10)	-8.6 (8)	2.6 (8)	-10.3 (9)
C22	14.1 (9)	17.2 (10)	23.4 (10)	-5.9 (8)	-0.4 (8)	-10.4 (8)
C23	21.1 (11)	27.7 (12)	35.5 (12)	-13.2 (9)	3.5 (9)	-20.8 (10)
C24	26.2 (11)	24.6 (12)	27.4 (11)	-14.2 (9)	0.6 (9)	-13.0 (9)
C25	40.8 (14)	36.9 (14)	31.0 (12)	-23.1 (11)	6.2 (10)	-17.8 (11)
C26	59.5 (17)	34.6 (14)	26.6 (12)	-27.4 (13)	-6.4 (12)	-4.9 (11)
C27	50.9 (16)	24.9 (13)	45.9 (15)	-13.9 (11)	-18.2 (13)	-4.9 (11)
C28	32.1 (13)	23.3 (12)	47.3 (14)	-7.6 (10)	-6.4 (11)	-15.4 (11)
C29	24.6 (11)	23.0 (11)	32.3 (12)	-10.5 (9)	-2.2 (9)	-13.9 (9)

Table S5. Hydrogen Atom Coordinates ($\text{\AA} \times 10^4$) and Isotropic Displacement Parameters ($\text{\AA}^2 \times 10^3$) for L3

Atom	X	y	z	U(eq)
H1	7161.9 (19)	3121.5 (14)	2770.4 (14)	21.6 (4)
H3	9869 (2)	297.2 (17)	778.4 (16)	21.7 (5)
H4	7470 (2)	1044.4 (17)	1577.6 (16)	21.3 (5)
H6	10127 (2)	2854.4 (17)	2525.8 (17)	21.4 (5)
H7	12515 (2)	2063.9 (17)	1753.6 (16)	20.9 (5)
H8a	5214 (2)	2247.9 (18)	1953.9 (17)	21.4 (5)
H8b	5655 (2)	1309.3 (18)	3234.1 (17)	21.4 (5)
H11	5928 (3)	1097.3 (18)	4965.6 (18)	27.3 (5)
H12	5458 (3)	512.9 (19)	6933.3 (18)	33.9 (6)
H13	3100 (3)	1444 (2)	7686.2 (19)	37.1 (6)
H14	1274 (3)	2986.8 (19)	6449.6 (18)	31.3 (6)
H16	429 (2)	4353.3 (17)	4433.9 (17)	23.7 (5)
H18	-474 (3)	5730.5 (18)	2434.8 (19)	30.0 (6)
H19	-24 (3)	6415.1 (19)	456.3 (19)	34.0 (6)
H20	2394 (3)	5577.7 (19)	-336.8 (19)	33.4 (6)
H21	4263 (3)	4031.6 (18)	850.7 (17)	25.3 (5)
H25	6045 (3)	5502 (2)	2146 (2)	39.5 (7)
H26	4118 (3)	7119 (2)	1021 (2)	47.3 (7)
H27	1989 (3)	8034 (2)	1914 (2)	49.4 (8)
H28	1807 (3)	7367 (2)	3922 (2)	39.6 (6)
H2	15270 (40)	570 (40)	400 (30)	131 (16)

Table S6. Multilevel analysis of the molecular structure of L3

Nº	Node degrees	Ω_i , %	Dimensionality of net	Topological type
1	10,16-c	1.11	3D	New topology with Point Symbol: {3 ²⁴ .4 ¹⁹ .5 ² } {3 ⁴² .4 ⁶¹ .5 ¹⁷ } ₂
2	10,13-c	2.04	3D	<u>10,13T91</u>
3	7-c	7.38	3D	bct/I 4/m m m->C 2/c (-a+b-2c,a+b,a-b; 1/4,1/4,1/4); Bond sets: <u>1,3,4,6,7,8:bct</u>
4	6-c	7.52	3D	<u>msw</u>
5	5-c	8.05	3D	<u>bnn</u>
6	3-c	8.99	2D	<u>hcb</u>
7	2-c	12.87	1D	<u>2C1</u>
8	12-c	15.16	0D	<u>1M2-1</u>

Table S7. Optimized geometrical parameters of L3

Parameter		Experimental	Parameter		Experimental
Bond length (Å)	B3LYP/6-311++G(d,p)		Bond angle (°)	B3LYP/6-311++G(d,p)	
O1-C5	1.2214	1.27	C5-O2-H42	105.8913	111.48
O2-C5	1.3672	1.28	H4-N3-C11	117.5461	119.08
O2-H42	0.9709	1.24	H4-N3-C16	117.691	119.10
N3-H4	1.0135	0.88	C11-N3-C16	123.559	121.81
N3-C11	1.3711	1.36	N3-H4-O43	169.9926	155.39
N3-C16	1.457	1.45	O1-C5-O2	120.7873	122.09
H4-O43	2.0903	2.15	O1-C5-C6	125.7466	118.91
C5-C6	1.4707	1.46	O2-C5-C6	113.4661	118.98
C6-C7	1.4033	1.39	C5-C6-C7	118.8126	121.44
C6-C14	1.4102	1.40	C5-C6-C14	122.7316	120.05
C7-H8	1.0853	0.95	C7-C6-C14	118.4558	118.49

C7-C9	1.3892	1.37	C6-C7-H8	118.5712	119.40
C9-H10	1.0841	0.95	C6-C7-C9	121.2813	121.29
C9-C11	1.4159	1.41	H8-C7-C9	120.1474	119.35
C11-C12	1.4188	1.41	C7-C9-H10	119.2326	119.82
C12-H13	1.086	0.94	C7-C9-C11	120.3699	120.35
C12-C14	1.3836	1.37	H10-C9-C11	120.3974	119.82
C14-H15	1.0844	0.95	N3-C11-C9	122.2322	122.23
O43-C44	1.232	1.22	N3-C11-C12	119.5457	119.35
C44-C45	1.4888	1.48	C9-C11-C12	118.2186	118.41
C44-C58	1.4898	1.48	C11-C12-H13	118.8463	119.83
C45-C46	1.4112	1.40	C11-C12-C14	120.7838	120.34
C45-C53	1.4014	1.38	H13-C12-C14	120.3697	119.82
C46-C47	1.4002	1.39	C6-C14-C12	120.8903	121.14
C46-C56	1.4923	1.48	C6-C14-H15	119.4509	119.43
C47-H48	1.0848	0.95	C12-C14-H15	119.6588	119.42
C47-C49	1.3941	1.37	O43-C44-C45	121.2551	121.01
			O43-C44-C58	120.7711	120.64
			C45-C44-C58	117.9734	118.33
			C44-C45-C46	120.9789	120.56
			C44-C45-C53	119.3399	119.98
			C45-C46-C56	121.227	121.10

		C47-C46-C56	119.0481	119.50
		C46-C47-H48	118.4252	119.75

Table S8. Calculated vibrational frequencies (cm^{-1}) assignments of L3 based on B3LYP/6–311++G(d,p) basis set

Mode No	Experimental wave number (cm^{-1})	Theoretical wave number (cm^{-1})		I_{IR}^{c}	$I_{\text{RAMAN}}^{\text{d}}$	Assignments (PED) ^(a,b)
		FT-IR	Unscaled			
192	3351	3631.52	3489.891	50.87	9.018704	γOH
191	3290	3572.24	3432.923	564.05	100	γNH
190	3110	3247.43	3120.78	4.78	0.847443	γCH
189	-	3242.08	3115.639	5.95	1.054871	γCH
188	-	3242.01	3115.572	10.22	1.811896	γCH
187	-	3238.82	3112.506	7.12	1.262299	γCH
186	-	3237.71	3111.439	0.9294	0.164773	γCH
185	-	3237.30	3111.045	10.63	1.884585	γCH
184	-	3236.30	3110.084	25.77	4.568744	γCH
183	-	3234.68	3108.527	16.91	2.997961	γCH
182	-	3224.94	3099.167	9.04	1.602695	γCH
181	-	3222.75	3097.063	12.02	2.131017	γCH
180	-	3219.91	3094.334	34.37	6.093431	γCH
179	-	3218.73	3093.201	34.51	6.118252	γCH
178	-	3217.10	3091.633	8.33	1.476819	γCH
177	-	3214.28	3088.923	5.75	1.019413	γCH
176	-	3208.11	3082.994	5.25	0.930769	γCH
175	-	3207.46	3082.369	4.20	0.744615	γCH

174	-	3202.04	3077.16	23.08	4.091836	γCH
173	-	3202.04	3077.16	2.74	0.485773	γCH
172	-	3190.36	3065.936	6.49	1.150607	γCH
171	-	3187.88	3063.553	3.36	0.595692	γCH
170	-	3184.30	3060.112	2.18	0.386491	γCH
169	-	3044.66	2925.918	21.65	3.838312	γCH
168	2852	3025.86	2907.851	45.54	8.073752	γCH
167	1750	1717.67	1650.681	309.36	54.8462	$\gamma\text{CO+}$ $\gamma\text{CC+}$ $\beta\text{HOC+}$ βHCC
166	-	1687.94	1622.11	10.56	1.872174	$\gamma\text{CC+}$ βHCC
165	1601	1683.56	1617.901	53.44	9.474337	$\gamma\text{CC+}$ $\gamma\text{CO+}$ βHCC
164		1680.11	1614.586	1.46	0.258842	$\gamma\text{CC+}$ βHCC
163	-	1672.31	1607.09	541.02	95.91703	$\gamma\text{CO+}$ $\gamma\text{CC+}$ $\beta\text{HCH+}$ $\beta\text{HCO+}$ βHCC
162	-	1667.26	1602.237	175.49	31.11249	$\gamma\text{CO+}$ $\gamma\text{CC+}$ βHCC
161	-	1649.31	1584.987	2.25	0.398901	$\gamma\text{CC+}$ βHCC
160	1550	1637.84	1573.964	1.12	0.198564	$\gamma\text{CC+}$ βHCC
159	-	1636.85	1573.013	95.57	16.94353	$\gamma\text{CC+}$ $\beta\text{HCN+}$ $\beta\text{HCC+}$ βHCH
158	-	1626.13	1562.711	345.36	61.22861	$\gamma\text{CO+}$ $\gamma\text{CC+}$ βHCC
157	-	1623.92	1560.587	2.13	0.377626	$\gamma\text{CO+}$ $\gamma\text{CC+}$ βHCC
156	-	1612.13	1549.257	21.90	3.882635	$\gamma\text{CO+}$ $\gamma\text{CC+}$ $\beta\text{HCC+}$ βHCH
155	-	1611.74	1548.882	53.13	9.419378	$\gamma\text{CO+}$ $\gamma\text{CC+}$ $\beta\text{HCC+}$ βHCH
154	-	1600.80	1538.369	3.26	0.577963	$\gamma\text{CC+}$ $\gamma\text{CN+}$ $\beta\text{HCC+}$ βHCH
153	-	1585.68	1523.838	217.61	38.57991	$\gamma\text{CC+}$ $\gamma\text{CN+}$ $\beta\text{HCC+}$ $\beta\text{HCH+}$ βOCO

152	1512	1584.27	1522.483	30.41	5.391366	γ_{CC+} β_{HCH+}	γ_{CN+} β_{OCO}	β_{HCC+}
151	1450	1556.74	1496.027	13.07	2.31717	γ_{CC} β_{HCH}	$+ \beta_{CNH+}$ β_{HCC+}	
143	1423	1484.60	1426.701	38.24	6.779541	γ_{CC+} β_{HCH}	β_{CNH+} β_{HCC+}	

Table S9. The values of calculated dipole moment $\mu(D)$, polarizability (α_0), first order hyperpolarizability, (β_{tot}) components of L3

Parameters	B3LYP/6-311++G(d,p)	Parameters	B3LYP/6-311++G(d,p)
μ_x	6.5518	β_{xxx}	341.9681
μ_y	0.0381	β_{yxx}	21.1670
μ_z	0.5198	β_{xyy}	-97.2962
$\mu(D)$	6.5725	β_{yyy}	-123.1739
α_{xx}	-268.8332	β_{zxx}	-36.0540
α_{xy}	22.9133	β_{xyz}	-22.5801
α_{yy}	-219.3266	β_{zyy}	22.8157
α_{xz}	-6.3929	β_{xzz}	16.9878
α_{yz}	-10.9098	β_{yzz}	9.2168
α_{zz}	-218.8156	β_{zzz}	10.1868
α_0 (e.s.u)	3.4×10^{-23}	β_{tot} (e.s.u)	2.398×10^{-30}

Table S10. Calculated energy values of L3 by B3LYP/6– 311++G(d,p) method

Parameter	Values
E_{Homo} (eV)	-5.51
E_{Lumo} (eV)	-1.86
Ionization potential	5.51
Electron affinity	1.86
Energy gap(eV)	3.64
Electronegativity	3.68
Chemical potential	-3.68
Chemical hardness	1.825
Chemical softness	0.547
Electrophilicity index	3.71

Table S11. Surface property information in Hirshfeld for L3

Mode	Minimum interaction	Mean interaction	Maximum interaction
D_{norm}	-0.787	0.599	2.364
D_i	0.563	1.774	3.620
D_e	0.563	1.799	3.694
Shape Index	-0.995	0.209	0.998
Curvedness	-3.625	-0.997	0.397

Fragment patches	0.0	9.5084	18.0000
-------------------------	-----	--------	---------

Table S12. 2-D finger print percentage of the total surface area for closed contact between atoms inside and outside the surface for L3

Atoms Surface %	O	N	H	C
O	-	-	17.6	0.4
N	-	-	0.4	-
H	17.6	0.4	47.4	29.4
C	0.4	-	29.4	4.9

Table S13. Hydrogen bonding and molecular docking with centromere associated protein inhibitor protein targets

S. No.	Protein (PDB ID)	No of residue	Bond distance (Å)	Inhibition Constant (micromolar)	Binding Energy (kcal/mol)	Refrence RMSD (Å)
1	5E1S	3	2.34	0.012	-10.8	6.396

References

- International Tables for X-Ray Crystallography, Vol. III, Kynoch Press, Birmingham, England, 1952.
- O. V. Dolomanov, L. J. Bourhis, R. J. Gildea, J. A. K. Howard and H. Puschmann, *J. Appl. Crystallogr.*, 42 (2009) 339–341.
- Blatov V. A., Shevchenko A. P., Proserpio D. M. Applied topological analysis of crystal structures with the program package ToposPro, *Cryst. Growth Des.*, 2014, 14, 3576–3586. doi: 10.1021/cg500498k
- O'Keeffe M., Peskov M. A., Ramsden S. J., Yaghi O. M. The reticular chemistry structure resource (RCSR) database of, and symbols for, crystal nets. *Acc. Chem. Res.*, 2008, 41, 1782–1789. doi: 10.1021/ar800124u
- Alexandrov E. V., Blatov V. A., Kochetkov A. V., Proserpio D.M. Underlying nets in three-periodic coordination polymers: topology, taxonomy and prediction from a computer-aided analysis of the Cambridge Structural Database. *CrystEngComm* 2011, 13, 3947-3958. doi: 10.1039/C0CE00636J
- Blatov V. A., Shevchenko A. P. Simplify to understand: how to elucidate crystal structures? *Struct. Chem.* 2021, doi: 10.1007/s11224-020-01724-4
- Alexandrov E. V., Shevchenko A. P., Blatov V. A. Topological Databases: Why Do We Need Them for Design of Coordination Polymers? *Cryst. Growth Des.* 2019, 19, 2604-2614. doi: 10.1021/acs.cgd.8b01721.
- G.A. Petersson, M.A. Al-Laham, *J. Chem. Phys.* **1991**, 94 (9), 6081.
- G.A. Petersson, A. Bennet, T.G. Tensfeld, M.A. Al-Laham, W.A. Shirley, J. Mantzaris, *J. Chem. Phys.* **1988**, 89(4), 2193.
- M.J. Frisch, et al., Gaussian 09, Revision E.01, Gaussian, Inc., Wallingford CT, 2009.
- F. Neese, *Mol. Sci.* **2012**, 2, 73.
- T. Lu. F. Chen, *J. Comp. Chem.* **2012**, 33, 580.
- A. Daina, O. Michielin, V. Zoete, *Scientific Reports*, **2017**, 7, 42717.
- Origin 8.0, OriginLab Corp., Northampton, MA.
- F.L. Hirshfeld, *Theor. Chim. Acta* **1977**, 44, 129–138.

16. M. A. Spackman, D. Jayatilaka, *Cryst. Eng. Comm.* **2009**, 11, 19–32.
17. W. Wang, Y. Ling, L. J. Yang, Q. L. Liu, Y. H. Luo, B. W. Sun, *Res. Chem. Intermed.* **2016**, 42 (4), 3157–3168.
18. D.A. Safin, K. Robeyns, Y. Garcia, *Cryst. Eng. Comm.* **2016**, 18, 7284- 7296.
19. N.P.G. Roeges, A Guide to the Complete Interpretation of the Infrared Spectra of Organic Structures, Wiley, New York, 1994. (b) N. Rekik, N. Issaoui, H. Ghalla, B. Oujia, M.J. Wojcik, Infrared spectral density of H-bonds within the strong anharmonic coupling theory: Indirect relaxation effect, *Journal of Molecular Structure* 844–845 (2007) 21–31.
20. P.S.Ganeshvar, M.Kanagaraj, S.Gunasekaran, T.Gnanasambandan. International J. of scientific & Engineering Research, Vol 7 (2016) ISSN 2229-5518.